Electric Power Components and Systems, 00:000–000, 2012

0731-356X / 12 $12.00 + .00

MIMO LQ Control of the Energy Production of a Synchronous Generator in a Nuclear Power Plant

Attila Fodor[a]

Attila Magyar[a]

Katalin M. Hangos[a,b]

[a] Department of Electrical Engineering and Information Systems,

University of Pannonia, 8200 Veszprém, Hungary

foa@almos.vein.hu and amagyar@almos.vein.hu

[b] Process Control Research Group, Computer and Automation Research

Institute HAS, Budapest, Hungary

hangos@sztaki.hu

A multiple-input multiple-output (MIMO) linear-quadratic (LQ) servo controller is proposed for a synchronous generator operating in a nuclear power plant that keeps the active power at the desired level and performs reactive power reference tracking using the reactive power demand from a central dispatch center. The controller design was based on the locally linearized version of a previous nonlinear dynamical model of the synchronous electrical generator [1], [2] the parameters of which have been identified using measured data from Paks Nuclear Power Plant (Hungary). The method can easily be applied to any industrial power plant generator connected to the electrical grid after estimating its parameters. The proposed observer based MIMO state feedback controller is a linear quadratic servo controller with very good reference tracking and disturbance rejection properties which were confirmed by simulation experiments.

Manuscript received in final form on March 14, 2014.

Address correspondence to A. Fodor.

1 Introduction

Nuclear power plants are important energy providers worldwide. They produce energy mainly in the form of electrical energy, the transportation and distribution of which is performed by using large-scale electrical power grids. This grid should be operated in a balanced way taking the time varying power demand of the consumers into account. Besides of the active power produced by a power plant, other characteristic variables of the produced energy are essential, most notably the reactive power and the frequency. The importance of the reactive power is indicated by the fact that insufficient reactive power of the system may result in voltage collapse. Therefore, it is widely accepted that the consumers of the reactive power should pay for it and the producers of the reactive power are enumerated [3]. Therefore, the power controllers of nuclear power plants should also take the production of the reactive power into account.

On the other hand, the presence of reactive power may cause overloading effects on the line, power breakers, transformers, relays and isolation elements, but it cannot be transformed into mechanical power. In addition, the presence of reactive power requires to increase the dimension of cables used in the transmission line. Therefore the management of reactive power generation and consumption is well investigated in the literature. A recent paper [4] proposes reactive power compensation using a fuzzy logic controlled synchronous machine (SM). Reactive power management is also a critical issue when dealing with the planning and operation of power networks. Its use for transmission line fault location and power system protection are described in [5].

From the viewpoint of the power grid the electric power generation of nuclear power is characterized by the operation of the electrical generators. This is caused by the fact that the final stage of the power production in a nuclear power plant (NPP) includes a synchronous generator (SG) that is driven by a turbine. A synchronous generator (SG) operating in a NPP and its controller is the subject of our study.

Because of the above described requirements on the operation of the large-scale electrical power grids, power plants should not only be able to follow the time-varying active and reactive power demand of the consumers and the central dispatch center, but also keep the quality indicators (frequency, waveform, total harmonic distortion) of the grid on the expected level. This can be achieved by applying proper control methods based on dynamic models of plant (see e.g. [6], [7]) and the involved generators.

Because of the specialties and great practical importance of the synchronous generators in power plants, their modeling for control purposes is also well investigated in the literature. Besides of the basic textbooks (see e.g. [1]) that describe the modeling, specialized papers are also available that use the developed models for the design of various controllers [8].

In addition to conventional control tasks related to synchronous generators in power plants, special purpose SG control studies are also reported. The behavior of a SG during short-circuit is investigated in [9]. This article reports the short-circuit characteristics of a stand-alone turbo-generator driven by separately excited DC motors, the applied model of the SG is similar to that used in this paper.

In a power system, voltage stability margin improvement can and should also be done by regulating generator voltages, transformer tap settings and capacitor

or reactor rated reactive powers. For this purpose, a reactive power rescheduling method with generator ranking has been proposed in [10].

The aim of this paper is to design a MIMO servo controller that keeps the active power of a SG in a real NPP at the desired level, and performs reactive power reference tracking using the reactive power demand from the central dispatch center. The design is based on our previously developed and validated nonlinear model of the SG [2] that has been locally linearized. Our earlier preliminary control study [11] has indicated that a MIMO LQ controller could be used for this purpose. The present paper reports the detailed controller design together with the verification of the controller using artificial step changes, and real local changing transients measured at the NPP. The controller design and verification methodology is intended to applied to any power plant generator connected to the electrical grid.

2 The power control problem in a pressurized water NPP

The Paks NPP, where the investigated generators work, is located in Hungary, and operates four pressurized water (VVER-440/213 type) reactors with a total nominal electrical power of 2000 MW. Each reactor is equipped with two turbine-generator units that work in parallel. The turbo generator is a specific synchronous generator with a special cooling system.

Our study is concerned with the power control of the Paks NPP. In this section a brief overview of the plant from the viewpoint of its synchronous generators is given first, then a description of the power changing operations is given.

2.1 The role of the SG in the plant technology

The SG is located in the secondary circuit of a unit in the Paks NPP. Every nuclear unit operates six steam generators with capacity 450 t/h on temperature 260 °C and pressure 46 bar that interface the primary and secondary circuits [12], [13], [14]. These six steam generators are connected to two turbo-generators, three to each. Every nuclear unit operates two independent secondary coolant circuits, that are controlled by independent control systems. The secondary coolant circuits begin with three steam generators that provide steam for the turbines. There are three turbines in each secondary coolant circuit (one high pressure and two low pressure ones), attached to one synchronous generator and one exciter machine set on the same axis.

2.2 The power control system

The power control of a unit in the Paks NPP is performed by three loosely coupled controllers: the power controller of the reactor, the turbine power controller and the generator exciter controller. While the reactor power controller is mainly responsible for taking care of the total power, the turbine controller regulates the frequency and the generator controller deals with maintaining the proper ratio of the active and reactive power.

The detailed model-based analysis of the reactor power controller of a unit in Paks NPP is reported in [15], that uses a simple dynamic model of the primary circuit based on first engineering principles.

As the generator controller operates relatively independently of the other two controllers involved in the power control, we aim at optimally re-design the generator controller using a simple control-oriented dynamic model in order to be able

to using a simple control-oriented dynamic model in order to be able to maintain the desired active and reactive power level even under power changing operation conditions.

2.3 Power changing operations

In Figure 1 the time varying output of a nuclear power plant, the Paks NPP is depicted during load changing transients. It can be seen that the reactive power (q_{out}) is also changing the same way as with the active power (p_{out}). Since a unit in the NPP of interest contains two generators, the same signals belonging to the two generators are both depicted.

It can be seen in Figure 1 that the reactive powers (q_{out}) of the SG are changing during the power switching. It can also be seen that the active power (p_{out}) of the generators follow the neutron flux of the reactor which follows the control rod position of the nuclear reactor.

In the case presented by Figure 1 the active power was controlled by a classical PI controller with the manipulated input being the exciter voltage (v_F). On the other hand, no reactive power control policy was used in the NPP, therefore the *reactive power follows the change of the active power.*

3 The model of the synchronous generator

In this section a state space model of a synchronous generator is presented. The model development is largely based on [1], [16] and [2] but the special circumstances of the generator operation in the considered NPP have also been taken into account. Only the basic steps of the model development and the resulting model equations

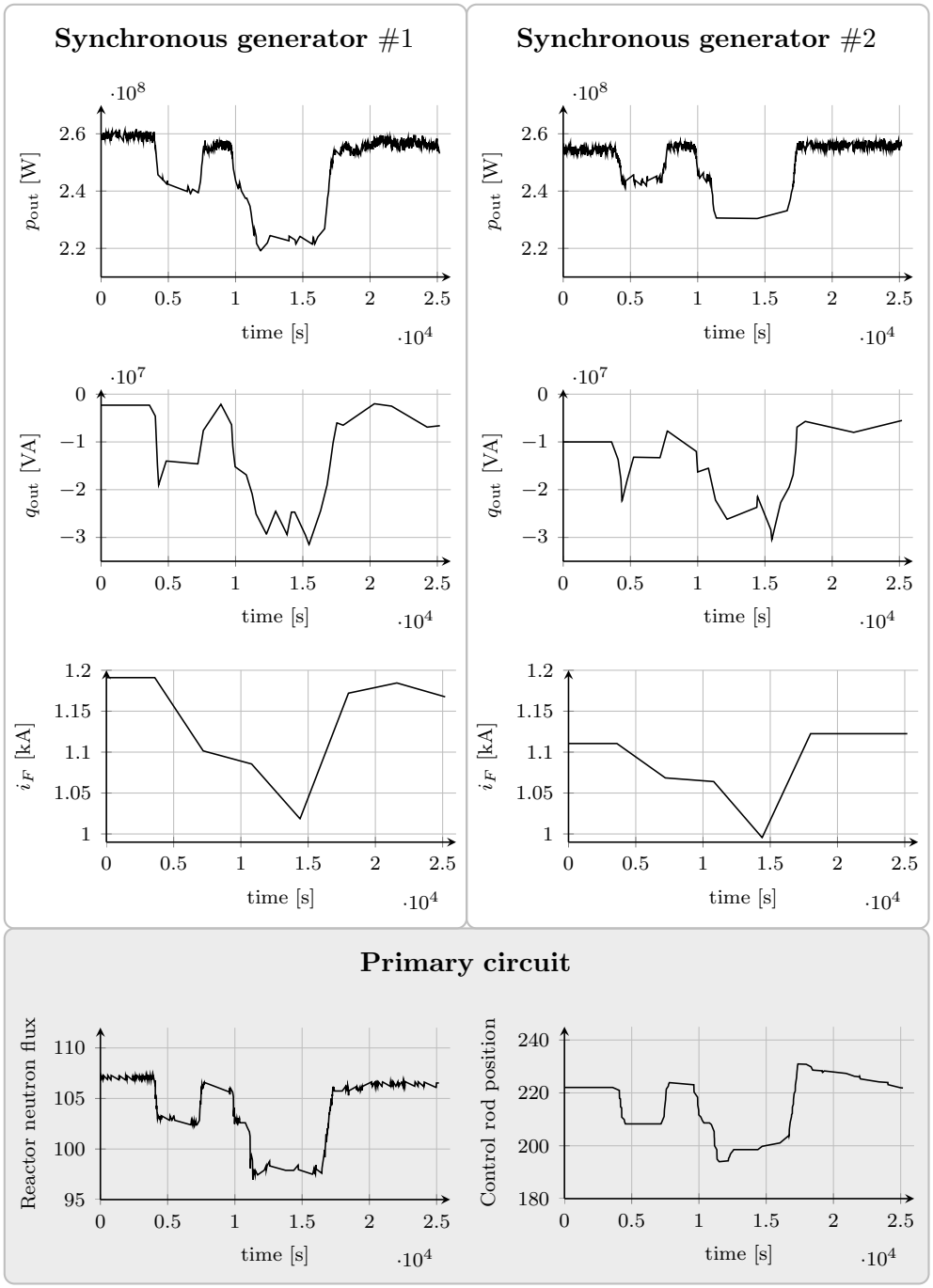

Figure 1: Effective and reactive power (p_{out} and q_{out}) and the exiting current (i_F) of two generators attached to the same reactor, the neutron flux and control rod position of the reactor during load changing transients. The close connection between the neutron flux and p_{out} is apparent. Because of the simple controller structure q_{out} follows p_{out}.

are described here using the notation list found in the Appendix. The detailed derivation together with the results of the model analysis can be found in [17], [18].

The SG model is based on the following simplification assumptions:

- a symmetrical three-phase stator winding system is assumed,
- one field winding is considered to be in the machine,
- there are two amortisseur or damper windings in the machine,
- all of the windings are magnetically coupled,
- the flux linkage of the winding is a function of rotor position,
- the copper loss and the slots in the machine can be neglected,
- the spatial distribution of the stator fluxes and apertures wave are considered to be sinusoidal,
- stator and rotor permeability are assumed to be infinite.

It is also assumed that all the losses due to wiring, saturation, and slots can be neglected.

The six windings (three stators, one rotor and two dampers) are magnetically coupled. Since the magnetic coupling between the windings is a function of the rotor position, the flux linkage of the windings is also a function of the rotor position. The actual terminal voltage v of the windings can be written in the form

$$v = \pm \sum_{j=1}^{J} (r_j \, i_j) \pm \sum_{j=1}^{J} \left(\frac{\mathrm{d}\lambda_j}{\mathrm{d}t} \right), \tag{1}$$

where i_j are the currents, r_j are the winding resistances, and λ are the flux linkages. The positive directions of the stator currents point out of the synchronous generator terminals.

Thereafter, the two stator electromagnetic fields, both traveling at rotor speed, can be identified by decomposing each stator phase current under steady state into

two components, one in phase with the electromagnetic field and another phase shifted by 90 °. With the above, we can construct an air-gap field with its maximal aligned to the rotor poles (d axis), while the other is aligned to the q axis (between poles) following the well-known method called Park's transformation. As a result of the derivation in [2] the vector voltage equation is as follows

$$\boldsymbol{v}_{dFDqQ} = -\boldsymbol{R_R}\,\boldsymbol{i}_{dFDqQ} - \boldsymbol{L}\,\frac{\mathrm{d}}{\mathrm{d}t}\boldsymbol{i}_{dFDqQ}, \tag{2}$$

with

$$\begin{aligned} \boldsymbol{v}_{dFDqQ} &= \begin{bmatrix} v_d & -v_F & v_D & v_q & v_Q \end{bmatrix}^T = \begin{bmatrix} v_d & -v_F & 0 & v_q & 0 \end{bmatrix}^T \\ \boldsymbol{i}_{dFDqQ} &= \begin{bmatrix} i_d & i_F & i_D & i_q & i_Q \end{bmatrix}^T, \end{aligned} \tag{3}$$

where v_d and v_q are the direct and the quadrature components of the stator voltage, v_D and v_Q are the direct and the quadrature components of the amortisseur windings voltage of the SG, i_d and i_q are the direct and the quadrature components of the stator current, i_D and i_Q are the direct and the quadrature components of the amortisseur windings current, while v_F and i_F are the exciter voltage and current. Furthermore, $\boldsymbol{R_R}$ and $\boldsymbol{L}$ are the following matrices

$$\boldsymbol{R_R} = \begin{bmatrix} r + R_e & 0 & 0 & \omega\, L_q & \omega\, k\, M_Q \\ 0 & r_F & 0 & 0 & 0 \\ 0 & 0 & r_D & 0 & 0 \\ -\omega\, L_d & -\omega\, k\, M_F & -\omega\, k\, M_D & r + R_e & 0 \\ 0 & 0 & 0 & 0 & r_Q \end{bmatrix} \tag{4}$$

and

$$\boldsymbol{L} = \begin{bmatrix} L_d + L_e & k\,M_F & k\,M_D & 0 & 0 \\ k\,M_F & L_F & M_R & 0 & 0 \\ k\,M_D & M_R & L_D & 0 & 0 \\ 0 & 0 & 0 & L_q + L_e & k\,M_Q \\ 0 & 0 & 0 & k\,M_Q & L_Q \end{bmatrix}, \tag{5}$$

where r is the stator resistance, r_F is the exciter resistance, r_D and r_Q are the direct and the quadrature part of the rotor resistance of the SG, L_d, L_q, L_D and L_Q are the direct and the quadrature part of the stator and rotor inductance, ω is the angular velocity, and M_F , M_D and M_Q are linkage inductances. The resistance R_e and inductance L_e represent the output transformer of the synchronous generator and the transmission line. The state-space model for the currents is obtained by expressing $\frac{\mathrm{d}}{\mathrm{d}t}\boldsymbol{i}_{dFDqQ}$ from (2), i.e.

$$\frac{\mathrm{d}}{\mathrm{d}t}\boldsymbol{i}_{dFDqQ} = -\boldsymbol{L}^{-1}\,\boldsymbol{R_R}\,\boldsymbol{i}_{dFDqQ} - \boldsymbol{L}^{-1}\,\boldsymbol{v}_{dFDqQ} \tag{6}$$

The purely electrical model (6) has to be extended with the equation (7) of rotational motion that gives the mechanical sub-dynamics, that is

$$\begin{aligned} \frac{\mathrm{d}\omega}{\mathrm{d}t} = &-\frac{L_d\,i_q}{3\tau_j}i_d + \frac{-k\,M_F\,i_q}{3\tau_j}i_F + \frac{-k\,M_D\,i_q}{3\tau_j}i_D + \frac{L_q\,i_d}{3\tau_j}i_q + \\ &\frac{k\,M_Q\,i_d}{3\tau_j}i_Q + \frac{-D}{\tau_j}\omega + \frac{T_{\mathrm{mech}}}{\tau_j}. \end{aligned} \tag{7}$$

Altogether, the state equations (6) and (7) have six state variables: i_d, i_F, i_D, i_q, i_Q and ω.

The manipulated input vector of the generator is $\boldsymbol{u} = \begin{bmatrix} v_F & T_{mech} \end{bmatrix}^T$, the disturbance input vector is $\boldsymbol{d} = \begin{bmatrix} v_d & v_q \end{bmatrix}^T$. Observe, that the state equations (6-7) are *bilinear in the state variables* because matrix $\boldsymbol{R_R}$ depends linearly on ω.

On the other hand, the effect of the generator is assumed to be negligible compared to that of the network on the network angular velocity. Then it follows that ω is constant, i.e. (7) can be replaced with its steady state version, which introduces an *algebraic constraint* that can be embedded in the remaining dynamics by solving it for ω:

$$\omega = \frac{1}{D} \cdot (-\frac{L_d}{3} i_d \, i_q - \frac{k \, M_F}{3} i_F \, i_q - \frac{k \, M_D}{3} i_D \, i_q + \frac{L_q}{3} i_q \, i_d + \frac{k \, M_Q}{3} i_Q \, i_d + T_{\text{mech}}). \tag{8}$$

The above expression is then substituted substituting it into the electrical dynamics (6). The obtained model has five state variables: i_d , i_F , i_D , i_q and i_Q [18]. This model is still nonlinear, inhibited from the mechanical sub-dynamics as the bi-linear expressions $i_q \, i_d$, $i_q \, i_F$, $i_q \, i_D$, $i_d \, i_Q$ now appear in matrix R (in equation (4)) and consequently in equation (6.)

The output active power equation can be written in the form

$$p_{\text{out}} = v_d \, i_d + v_q \, i_q, \tag{9}$$

and the reactive power is

$$q_{\text{out}} = v_d \, i_q - v_q \, i_d. \tag{10}$$

where v_d and v_q are disturbances and the currents are measured state variables Equations (9-10) are the *output equations* of the generator's state space model. The *performance outputs* (11) of the generator are the active and reactive power since these two signals should be able to track the demand (i.e. reference signal) of the central dispatch center.

$$\boldsymbol{y}_{\text{perf}} = \begin{bmatrix} p_{\text{out}} & q_{\text{out}} \end{bmatrix}^T \tag{11}$$

Parameter	Value (p.u.)	Parameter	Value (p.u.)
r	0.0211	M_R	1.5500
R_e	0.0000	L_d	1.2100
r_F	0.0006	L_q	1.5260
r_D	0.0131	L_e	0.0000
r_Q	0.0540	L_F	1.6510
k	1.2247	L_D	1.6050
M_F	1.2656	L_Q	1.5260
M_D	1.2656	τ_j	1786.0
M_Q	1.2468	D	2.0040

Table 1: Parameters of the synchronous generator model

Note, that *performance output equations are bilinear in the state and input variables*. It is convenient to define the measurable/computable state variables of the system (i_d, i_F, and i_q) to be the measured outputs of the system, i.e.

$$\boldsymbol{y}_{\text{meas}} = \begin{bmatrix} i_d \; i_F \; i_q \end{bmatrix}^T .$$

The model parameters have been estimated by using measured data of a sufficiently exciting load changing transient from the synchronous generator operating in the Paks NPP. The estimated parameters of the SG are dimensionless (p.u.) [2], they are collected in Table 1.

The quality of the model has also been evaluated by the fit in the active and reactive power in [2], and a good fit could be achieved.

3.1 The locally linearized model of the synchronous generator

The steady-state values of the state variables can be obtained from the steady-state version of state equation (6) extended with the algebraic constraint defined by the steady state version of (7) using the above parameters. The equilibrium point of the system is found to be

$$\begin{bmatrix} i_d^0 \; i_q^0 \; i_F^0 \; i_D^0 \; i_Q^0 \end{bmatrix}^T = \begin{bmatrix} -1.75 \; 0.79 \; 2.98 \; 1.24 \cdot 10^{-7} \; 7.18 \cdot 10^{-8} \end{bmatrix}^T \tag{12}$$

The locally linearized state-space model has the form of (14), where the state vector $\boldsymbol{x}$ is the centered version of the nonlinear models state vector, i.e.

$$\boldsymbol{x}^T = \begin{bmatrix} i_d - i_d^0 \; i_q - i_q^0 \; i_F - i_F^0 \; i_D - i_D^0 \; i_Q - i_Q^0 \end{bmatrix}^T. \tag{13}$$

The two distinct output equations stand for the performance output and the measured output, respectively.

$$\begin{aligned} \frac{\mathrm{d}\boldsymbol{x}}{\mathrm{d}t} &= \boldsymbol{A}\,\boldsymbol{x} + \boldsymbol{B_u}\,\boldsymbol{u} + \boldsymbol{B_d}\,\boldsymbol{d} \\ \boldsymbol{y}_{\mathrm{meas}} &= \boldsymbol{C}_{\mathrm{meas}}\,\boldsymbol{x} \\ \boldsymbol{y}_{\mathrm{perf}} &= \boldsymbol{C}_{\mathrm{perf}}\,\boldsymbol{x} + \boldsymbol{D_u}\,\boldsymbol{u} + \boldsymbol{D_d}\,\boldsymbol{d} \end{aligned} \tag{14}$$

The matrices $\boldsymbol{A}, \boldsymbol{B_u}, \boldsymbol{B_d}, \boldsymbol{C}_{\mathrm{meas}}, \boldsymbol{C}_{\mathrm{perf}}, \boldsymbol{D_u}$ and $\boldsymbol{D_d}$ are constants.

4 Observer based LQ-servo control of the synchronous generator

The advanced control design of the synchronous generators of power plants is far from being trivial because of the nonlinearity of the generator and the widely varied power demand of the consumers (see e.g. [19], [20], or [21] for recent studies). The control aims and expectations against the controller can be summarized as follows.

- The performance output ($\boldsymbol{y}_{\mathrm{perf}}$) of the system should follow the prescribed time varying piecewise constant reference signal.

- The closed loop system should be locally asymptotically stable.
- The performance output ($\boldsymbol{y}_{\text{perf}}$) should be insensitive with respect to disturbance $\boldsymbol{d}$.

The above aims suggest the use of LQ-servo technique for the controller design [22]. The choice is justified by the following properties of the LQ-servo method.

- It is a robust method, i.e. relatively insensitive for the difference between the linear and nonlinear models, moreover it performs trajectory tracking that was the primary control aim.
- It has good disturbance rejection properties.

A previous paper [11] presented a prototype LQ controller for the above aims, however, its tracking and robustness performance is far from acceptable in real industrial applications. As an additional aim, the controller designed in the sequel has to cope industrial conditions which should be justified by controller verification using real measurement data from Paks NPP.

As an LQ-servo controller applies full state feedback and not all of the state variables are measurable, the need of designing a state observer [23], [24] arises.

4.1 State observer design

The primary task of the observer is to determine the estimated value of the state vector $\boldsymbol{x}_{\text{obs}}$ from the measured output $\boldsymbol{y}_{\text{meas}}$. The observer is designed by pole placement technique using the system parameters $\boldsymbol{A}$, $\boldsymbol{B_u}$ and $\boldsymbol{C}_{\text{meas}}$. The poles λ_{obs} of the observer error dynamics are designed to be faster (15) than the locally linearized system's poles in order that the error transients decay faster than the

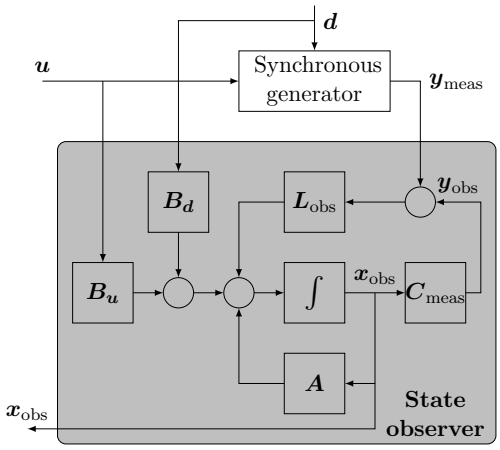

Figure 2: State observer structure for the synchronous generator

system transients. The poles of the observer are chosen to be

$$\lambda_{\text{obs}} = \begin{bmatrix} -5 & -6 & -7 & -8 & -10 \end{bmatrix}^{\mathbf{T}}. \tag{15}$$

The observer structure can be seen in Figure 2, the observer gain matrix $\boldsymbol{L}_{\text{obs}}$ has the following value

$$\boldsymbol{L}_{\text{obs}} = \begin{bmatrix} 12.1913 & -1.4484 & -10.3415 & 8.5417 & -39.2208 \\ 0.3850 & 7.6033 & 1.1784 & 7.9901 & -5.1052 \\ 0.1961 & 0.0263 & 8.1142 & 14.9986 & -13.4230 \end{bmatrix} \tag{16}$$

4.2 LQ servo controller design

The LQ-servo control itself is based on the extension of the linear model (14) with a tracking error variable $\boldsymbol{z}$ that represents the difference between the reference input $\boldsymbol{r}$ and the performance output $\boldsymbol{y}_{\text{perf}}$. The extended state equation has the form (17)

$$\begin{aligned} \frac{\mathrm{d}\boldsymbol{x}}{\mathrm{d}t} &= \boldsymbol{A}\,\boldsymbol{x} + \boldsymbol{B}_{\boldsymbol{u}}\,\boldsymbol{u} + \boldsymbol{B}_{\boldsymbol{d}}\,\boldsymbol{d} \\ \frac{\mathrm{d}\boldsymbol{z}}{\mathrm{d}t} &= \boldsymbol{r} - \boldsymbol{y}_{\text{perf}} = \boldsymbol{r} - \boldsymbol{C}_{\text{perf}}\,\boldsymbol{x} - \boldsymbol{D}_{\boldsymbol{u}}\,\boldsymbol{u} - \boldsymbol{D}_{\boldsymbol{d}}\,\boldsymbol{d} \end{aligned}. \tag{17}$$

The extended state equation in block matrix form is given by equation (18) below where $\tilde{\boldsymbol{x}} = \begin{bmatrix} \boldsymbol{x} \ \boldsymbol{z} \end{bmatrix}^T$

$$\frac{\mathrm{d}\tilde{\boldsymbol{x}}}{\mathrm{d}t} = \begin{bmatrix} \boldsymbol{A} & \boldsymbol{0} \\ -\boldsymbol{C}_{\mathrm{perf}} & \boldsymbol{0} \end{bmatrix} \tilde{\boldsymbol{x}} + \begin{bmatrix} \boldsymbol{B_u} \\ -\boldsymbol{D_u} \end{bmatrix} \boldsymbol{u} + \begin{bmatrix} \boldsymbol{B_d} \\ -\boldsymbol{D_d} \end{bmatrix} \boldsymbol{d} + \begin{bmatrix} \boldsymbol{0} \\ \boldsymbol{I} \end{bmatrix} \boldsymbol{r} \ . \tag{18}$$

The structure of the LQ-servo control loop can be seen in Figure 3, where the inner loop is the stabilizing state feedback controller, and the outer integrating loop implements the reference tracking (servo) control.

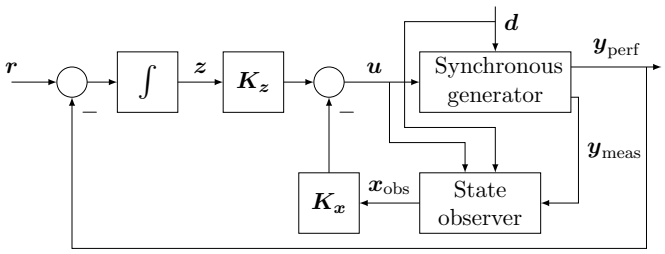

Figure 3: Observer based LQ-servo controller structure

As in the case of LQR design, the objective function to be minimized with respect to (18) is a functional of the form

$$J(\tilde{\boldsymbol{x}}, \boldsymbol{u}) = \int_0^\infty (\tilde{\boldsymbol{x}}^T \boldsymbol{Q}\, \tilde{\boldsymbol{x}} + \boldsymbol{u}^T \boldsymbol{R}\, \boldsymbol{u})\, \mathrm{d}t. \tag{19}$$

The design parameters of the LQ controller design method are the positive definite symmetric quadrature matrices $\boldsymbol{Q}$ and $\boldsymbol{R}$, where $\boldsymbol{Q}$ penalizes the state, and $\boldsymbol{R}$ penalizes the input variable. Of course, the compromise between the state signal norm (tracking quality of the control) and the input signal norm (cheapness of the control) has to be found. The state and input penalty factors were chosen to be

$$\begin{aligned} \boldsymbol{Q} &= 100\,\mathrm{diag}\begin{bmatrix} 1 & 1 & 1 & 1 & 1 & 100 & 10 \end{bmatrix}, \\ \boldsymbol{R} &= \mathrm{diag}\begin{bmatrix} 1 & 1 \end{bmatrix}. \end{aligned} \tag{20}$$

The last two diagonal elements of $\boldsymbol{Q}$ in (20) are the penalties of the tracking error variable $\boldsymbol{z}$. The feedback gain that minimizes (19) with respect to (18) and governs the extended system to its equilibrium is in block matrix form $\boldsymbol{K} = \begin{bmatrix} \boldsymbol{K_x} & \boldsymbol{K_z} \end{bmatrix}$ with numerical values (21).

$$\begin{aligned} \boldsymbol{K_x} &= \begin{bmatrix} -401.3310 & -378.4688 & -375.2029 & 119.7380 & 138.7553 \\ -252.8653 & -174.3798 & -174.6745 & 38.8057 & 68.5166 \end{bmatrix}, \\ \boldsymbol{K_z} &= \begin{bmatrix} -99.6438 & -2.6667 \\ -8.4329 & 31.5101 \end{bmatrix}. \end{aligned} \tag{21}$$

4.3 LQ servo controller verification

In order to verify the designed controller the transient response and the tracking properties have been checked.

4.3.1 Verification using step signals During the normal operation of the NPP, step-type reference changes are used according to the load changes between day and night operation. Therefore the active power reference tracking experiments have been performed using step signals. The result of the time domain analysis can be seen in Figure 4, where the transient response and reference tracking of p_{out}, and q_{out} is apparent. The reference of q_{out} was chosen to be constant zero. It can be clearly seen that the MIMO controller enables the treatment of active and reactive power independently (to some extent), as opposed to the original PI control scheme (Figure 1). The controller's robustness with respect to realistic (step-type) changes in the disturbance signal $\boldsymbol{d}$ has also been examined; the LQ-servo compensates the step-type disturbances at time 250 and time 450 satisfactorily. The closed loop system's local asymptotic stability is guaranteed by the LQ method.

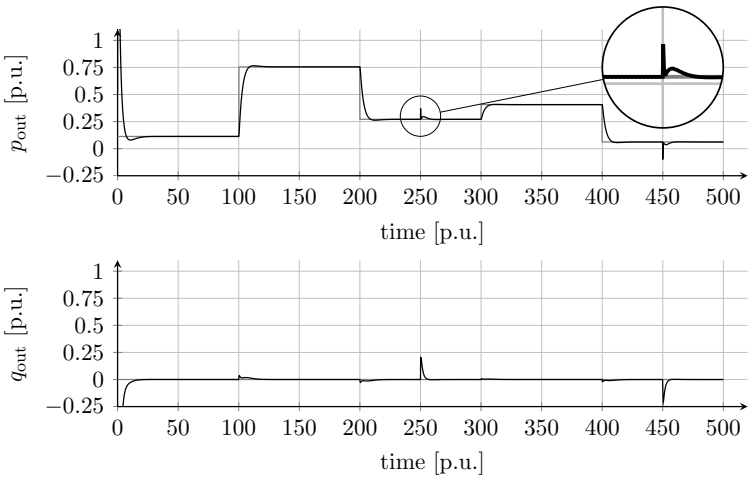

Figure 4: Transient response and reference tracking of active and reactive power. The disturbance rejection properties have also been examined using step-like changes of the disturbances v_d and v_q at time 250 (highlighted) and time 450, respectively.

4.3.2 Verification using measured data The measured data of the generator #1 in Figure 1 were used for verification in such a way that the active power reference signal was set equal to the measured one, and the reactive power reference was to be zero.

The simulation results using measured data are shown in Figure 5, where the controller generated active (p_{out}) and reactive (q_{out}) power are shown. It is apparent that the designed controller has an excellent fit with both the simulated active and reactive power signal. The measured input data of the generator contains the effect of the disturbance by the infinite huge electrical network, but this disturbance apparently does not influence the stability of the designed LQ controller.

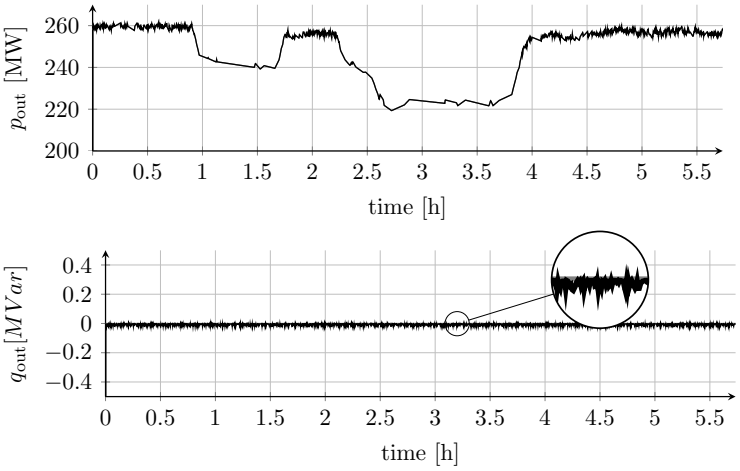

Figure 5: Transient response and reference tracking of active and reactive power on valid data from Paks NPP.

5 Conclusion and further work

In this work an LQ-type multiple-input multiple-output controller has been presented that does not only control active power of a synchronous generator, but can follow the reactive power demand, as well. This fits well into the recent trends in electrical energy market, where it is more widely accepted that consumers pay for the reactive power support service.

The developed controller is based on a locally linearized model of the SG operating in the Paks NPP, and applies a state observer for its realization. The proposed controller was verified by simulation using artificial step changes and real load changing signals, and good tracking and robustness properties were observed.

The proposed method can easily be applied to any industrial power plant generator connected to the electrical grid, if one follows the parameter estimation procedure suggested in [2] that only uses passive transient measured data.

Further work includes the investigation of the interplay between the power controller of the plant and the designed LQ-servo controller of the generator to further increase their adaptivity and efficiency.

References

[1] P. Anderson, and A. Fouad, Power-Systems-Control and Stability, The IOWA State University Press, Ames Iowa, USA, 1977.

[2] A. Fodor, A. Magyar, and K. M. Hangos, Control-Oriented Modeling of the Energy-Production of a Synchronous Generator in a Nuclear Power Plant, *Energy*, Vol. 39, 2012, pp. 135–145.

[3] M. Dittmar, Nuclear energy, Status and future limitations, *Energy*, Vol. 37(1), 2012, pp. 35–40.

[4] I. Colak, R. Bayindir, and O. Bay, Reactive power compensation using a fuzzy logic controlled synchronous motor, *Energy Convers Manage* 2003, Vol. 44, pp. 2189–2204

[5] W. Xiu, and Y. Liao, Accurate Transmission Line Fault Location Considering Shunt Capacitances Without Utilizing Line Parameters, *Electric Power Components and Systems*, Vol. 39:16, 2011, pp. 1783-1794

[6] R. N. Banavar, and U. V. Deshpande, Robust controller design for a nuclear power plant using H-infinity optimization, *Proc. of the 35th Conference on Decision and Control*, Kobe, Japan, 1996, pp. 4474-4479.

[7] M.G. Na, D.W. Jung, S.H. Shin, J.W. Jang, K.B. Lee and Y.J. Lee, A model predictive controller for loadfollowing operation of PWR reactors. *IEEE Transactions on Nuclear Science*, (52), 2005, pp. 1009-1020.

[8] F. de Mello, and C. Concordia, Concepts of synchronous machine stability as affected by excitation control, *IEEE Transactions on Power Apparatus and Systems PAS-*

88 (4), 1969, pp. 316–329.

[9] S. O. Emeka, Dynamics of a Turbo-generator Driven by DC Motors During Off-line Three-phase Sudden Short Circuit, *Electric Power Components and Systems*, 2011, Vol. 39:16, pp. 1828–1844

[10] H. Raoufi, and M. Kalantar, Reactive power rescheduling with generator ranking for voltage stability improvement, *Energy Convers Manage*, 2009, Vol. 50, pp. 1129–1135

[11] A. Fodor, A. Magyar, and K. M. Hangos, MIMO LQ Control of the Energy Production of a Synchronous Generator in a Nuclear Power Plant, *Chemical Engenieering Transactions*, 2012, Vol. 29, pp. 361–366

[12] Sz. Rozgonyi and K.M. Hangos, Domain of attraction analysis of a controlled hybrid reactor model, Annals of Nuclear Energy, (38), 2011, pp. 969–975.

[13] Cs. Fazekas, G. Szederkényi, and K.M. Hangos, A simple dynamic model of the primary circuit in VVER plants for controller design purposes, *Nuclear Engineering and Design*, Vol. 237, 2007, pp. 1071-1087.

[14] IAEA. Pressurized water reactor simulator, *IAEA-TCS-22*, ISSN 1018-5518, IAEA, Vienna, 2003.

[15] K. M. Hangos, J. Bokor, G. Szederkényi, Analysis and Control of Nonlinear Process Systems, Springer, 2004.

[16] K. M. Hangos, and I. Cameron, Process modelling and model analisys, Academic Press, London, 2001.

[17] A. Fodor, A. Magyar, and K. M. Hangos, Dynamic modeling and analysis of a synchronous generator in a nuclear power plant, *10th International PhD Workshop on Systems and Control*, Hluboka nad Vltavou, Czech Republic, ISBN:978-80-903834-3-2, 2009, pp. 91–96.

[18] A. Fodor, A. Magyar, and K. M. Hangos, Dynamic modeling and model analysis of a large industrial synchronous generator, *IEEE Applied Electronics*, Pilsen, Czech

Republic, 2010, pp. 91–96.

[19] A. Leon, J. Solsona, J. Figueroa, and M. Valla, Optimization with constraints for excitation control in synchronous generators, *Energy*, Vol. 36 (8), 2011, pp. 5366–5373.

[20] L. Fernandez, C. Garcia, and F. Jurado, Comparative study on the performance of control systems for doubly fed induction generator (DFIG) wind turbines operating with power regulation, *Energy*, Vol. 33 (9), 2008, pp. 1438–1452.

[21] M. Boroushaki, M. B. Ghofrani, C. Lucas, and M. J. Yazdanpanah, An intelligent nuclear reactor core controller for load following operations, using recurrent neural networks and fuzzy systems, *Annals of Nuclear Energy*, 2003, Vol. 30, pp. 63-80

[22] M. A. Athans, and P. L. Falb, Optimal Control, McGraw-Hill, New York, 1966.

[23] G. Wozny, G. Fieg, L. Jeromin, and H. Gülich, Design and analysis of a state observer for the temperature front of a retification column, *Chemical Engineering and Technology* 12(1), 1989, pp. 339–344.

[24] R. Neimeier, G. Schulz-Ekloff, T. Vielhaben, and G. Thiele, A nonlinear observer for the iron-catalysed hydrogen peroxide decomposition in a continuous stirred tank reactor, *Chemical Engineering and Technology*, Vol. 20(6), 1997, pp. 391–395.

6 Appendix

Abbreviations

APPS	Asynchronous Parallel Pattern Search
LQ, LQR	Linear-quadratic, Linear-quadratic Regulator
MIMO	Multiple-input multiple-output
NPP	Nuclear power plant
p.u.	Per Unit, Base quantities
SG and SM	Synchronous generator and Synchronous machine

Symbols

$\boldsymbol{A}, \boldsymbol{B_u}, \boldsymbol{B_d}, \boldsymbol{C}_{\text{meas}}$ $\boldsymbol{C}_{\text{perf}}, \boldsymbol{D_u}, \boldsymbol{D_d}$	State space matrices of the synchronous generator
$\boldsymbol{d}$	Disturbances of the SG
D and H	Damping and Inertia constant
$\boldsymbol{I}$	Unit matrix
i_d and i_q	Stator voltage, d and q component
i_D and i_Q	Currents of amortisseur winding
i_{out}	Stator current
$J(\tilde{\boldsymbol{x}}, \boldsymbol{u})$	Object function of the LQ controller
$k = \sqrt{3/2}$	Constant
$\boldsymbol{K}$	Feedback gain matrix
λ_{obs}	The poles of the observer
$L_{AD} = k\, M_D$	Amortisseur winding linkage inductance
$L_{AF} = k\, M_F$	Field linkage inductance
$L_{AQ} = k\, M_Q$	Amortisseur winding linkage inductance
L_{AD} and L_{AQ}	Mutual inductances
L_d and L_q	d and q component of stator inductance
L_D and L_Q	Inductances of amortisseur winding
$\boldsymbol{L}_{\text{obs}}$	Observer gain matrix
l_d and l_q	Linkage inductances
l_F, l_D and l_Q	Linkage inductances
L_{FB}	Rotor inductance, base
L_{MD} and L_{MQ}	Mutual inductances
M_D, M_Q and M_F	Mutual inductances
r	Stator resistance

R_e and L_e	Line resistance and inductance
r_F, r_D and r_Q	Rotor resistances
p_{out} and q_{out}	Active and Reactive power
$\boldsymbol{Q}$ and $\boldsymbol{R}$	State and input penalty factors of the controller
T_{mech}	Mechanical torque
v_d and v_q	Stator voltage, d and q component
v_F and i_F	Exciter voltage and current
$\boldsymbol{y}_{\text{perf}}$	Performance outputs of the synchronous generator
$\boldsymbol{y}_{\text{meas}}$	Measured outputs of the synchronous generator
ω	Angular velocity
ω_B	Angular velocity, base
$\tau_j = 2\,H\,\omega_B$	Inertial time constant

$$\boldsymbol{A} = 10^{-3} \cdot \begin{bmatrix} -26.872 & 0.3249 & 10.564 & -2201.5 & -1947.7 & -1727.4 \\ 9.26216 & -4.914 & 78.448 & 758.746 & 671.266 & 595.345 \\ 17.008 & 4.4313 & -94.124 & 1393.33 & 1232.69 & 1093.27 \\ 11628.1 & 7836.3 & 7836.35 & -106.52 & 272.907 & 2935.78 \\ -11635.7 & -7841.5 & -7841.5 & 106.585 & -308.47 & -2937.7 \\ -0.0841 & -0.2272 & -0.2272 & -0.6738 & -0.5001 & -1.1221 \end{bmatrix}$$

$$\boldsymbol{B_d} = \begin{bmatrix} -1.2742 & 0 \\ 0.4391 & 0 \\ 0.8064 & 0 \\ 0 & -5.0505 \\ 0 & 5.0538 \end{bmatrix} \quad \boldsymbol{B_u} = \begin{bmatrix} 0.4391 & -0.8620 \\ -6.6400 & 0.2971 \\ 5.9884 & 0.5455 \\ 0 & 1.4650 \\ 0 & -1.4659 \end{bmatrix}$$

$$\boldsymbol{C}_{\text{meas}} = \begin{bmatrix} 1\,0\,0\,0\,0 \\ 0\,1\,0\,0\,0 \\ 0\,0\,0\,1\,0 \end{bmatrix} \quad \boldsymbol{C}_{\text{perf}} = \begin{bmatrix} -0.6600 & -0.2804 \\ 0 & 0 \\ 0 & 0 \\ 0.2804 & -0.6600 \\ 0 & 0 \end{bmatrix}^T$$

$$\boldsymbol{D_d} = \begin{bmatrix} -0.8774 & 0.3927 \\ 0.3927 & 0.8774 \end{bmatrix} \quad \boldsymbol{D_u} = \begin{bmatrix} 0\,0 \\ 0\,0 \end{bmatrix}$$

Acknowledgment

We acknowledge the financial support of this work by the Hungarian State and the European Union under the TAMOP-4.2.2.A-11/1/ KONV-2012-0072 project. This work was also supported in part by the Hungarian Research Fund through grant 83440.